Int. J. Electrochem. Sci., 8 **(2013)** 6851 - 6863

International Journal of
ELECTROCHEMICAL
SCIENCE
www.electrochemsci.org

Initial Corrosion of Pure Zinc Under NaCl Electrolyte Droplet Using a Zn-Pt-Pt Three-Electrode System

Shanhua Song[1,2], *Zhuoyuan Chen*[*,1]

[1] National Engineering Research Center for Marine Corrosion Protection, Institute of Oceanology, Chinese Academy of Sciences, 7 Nanhai Road, Qingdao 266071, China
[2] University of Chinese Academy of Sciences, 19 (Jia) Yuquan Road, Beijing 100039, China
[*]E-mail: zychen@qdio.ac.cn

Received: 19 March 2013 / *Accepted:* 13 April 2013 / *Published:* 1 May 2013

A three-electrode system was developed and employed to investigate the initial corrosion of pure zinc under a NaCl electrolyte droplet by using potentiodynamic polarisation and electrochemical impedance spectroscopy. The configuration of this proposed electrode system can minimise resistance polarisation. Thus, it can be used to investigate the atmospheric corrosion of zinc covered with a thin-electrolyte layer. Both the curve-fitting method and the method of combining linear polarisation with pre-Tafel region of polarisation are in accordance for the data analysis of the polarisation curves in the vicinity of corrosion potential. The data from electrochemical impedance spectroscopy corroborate those from the polarisation curves in the vicinity of corrosion potential.

Keywords: zinc; electrochemical impedance spectroscopy; polarization; atmospheric corrosion; NaCl electrolyte droplet

1. INTRODUCTION

Zinc is a very important anti-corrosion material and it has been extensively used as a coating for metals and as sacrificial anodes and paint pigments because of its relatively lower corrosion potential (E_{corr}) in the electrochemical series. A large proportion of all zinc, perhaps more than a third, is used to galvanize metals such as iron to prevent corrosion. Galvanized metals, especially galvanized steel, are most commonly used for structures and products that are exposed to atmospheric environments. Because of its widespread practical application, much work concerning the atmospheric corrosion of zinc material has been performed both in field and in controlled laboratory exposures [1-5].

Sodium chloride (NaCl), which is mainly from the ocean, is probably one of the most important

salt particles for atmospheric corrosion and it can be used as a corrosion stimulator in accelerated tests of metals exposed to marine environments. Due to its importance, much work has been done in recent decades to explore the effect of NaCl particles on the atmospheric corrosion of metals [6-10].

The thin-film electrolyte absorbed on the metal surface normally does not distribute evenly and often forms different-sized water droplets on the metal surface because of the effect of surface energy. Understanding the corrosion behaviours of zinc under an electrolyte droplet is very important. Neufeld *et al* [6] studied the initial corrosion of zinc under a NaCl electrolyte droplet and a secondary spreading effect was observed from the periphery of the droplet. Chen *et al* [7] reported that the secondary spreading effect of the NaCl electrolyte was strongly dependent on the CO_2 and SO_2 content of the introduced humid air. Ambient level of CO_2 (350 ppm) resulted in a relatively low spreading effect, whereas the lower level of CO_2 (<5 ppm) caused a much faster spreading over a larger area. In the presence of SO_2, the secondary spreading effect was absent. Muster *et al* [11] investigated the influence of droplet characteristics on the atmospheric corrosion of zinc using a multi-microelectrode approach. Tsuru *et al* [12] found that tiny water micro-droplets were formed on the spreading wet area of the NaCl electrolyte droplet on carbon steel. The formation of these micro-droplets depended on both the cation of the salt and the corrosion of the steel substrate.

The exploration of testing methods for the evaluation of atmospheric corrosion is still causing widespread concern in the research community. Electrochemical test methods are very important for corrosion science because they are normally very simple and quick [13]. However, their applications in atmospheric corrosion are very challenging. Yee *et al* [14] measured the potential profiles using a scanning Kelvin microprobe and developed a celebrated equation to describe the relationship between the Volta potential and E_{corr}. Nishikata *et al* [15] measured the electrochemical impedance spectroscopy (EIS) of stainless steel and copper covered with thin-electrolyte layers and performed the numerical analysis of the transmission line model. They pointed out that the EIS is very useful for the mechanistic study of atmospheric corrosion. Liao *et al* [16] investigated the corrosion behavior of copper under chloride-containing thin-electrolyte layers using cathodic polarisation, EIS and linear polarisation. They discussed the effect of electrolyte layer thickness on the corrosion rate and proposed a corrosion model. Dubuisson *et al* [8] for the first time designed and built a micro-reference and counter electrode (CE) using two Platinum (Pt) wires and inserted it into the electrolyte drop on zinc surface to study the polarisation resistance (R_p) and the proportionality constant of the Stern and Geary equation. They found that the corrosion rate of zinc increased with the decrease of the thickness of the electrolyte drop.

Although numerous studies have been conducted on the atmospheric corrosion of zinc, key questions still exist regarding the corrosion behaviours of a NaCl-contaminated zinc surface exposed to humid air. The goal of the current study was to investigate the effects of NaCl particles on the initial atmospheric corrosion of zinc. In this paper, the authors developed a three-electrode cell system (Zn-Pt-Pt). The benefit of this three-electrode system is that it can be used for an in-situ electrochemical study on the atmospheric corrosion of zinc covered with a thin-electrolyte layer with several micrometres in thickness. The authors studied the feasibility of using Pt as a reference electrode (RE) and the initial corrosion behaviours of zinc under a NaCl droplet by using electrochemical test methods.

2. EXPERIMENTAL

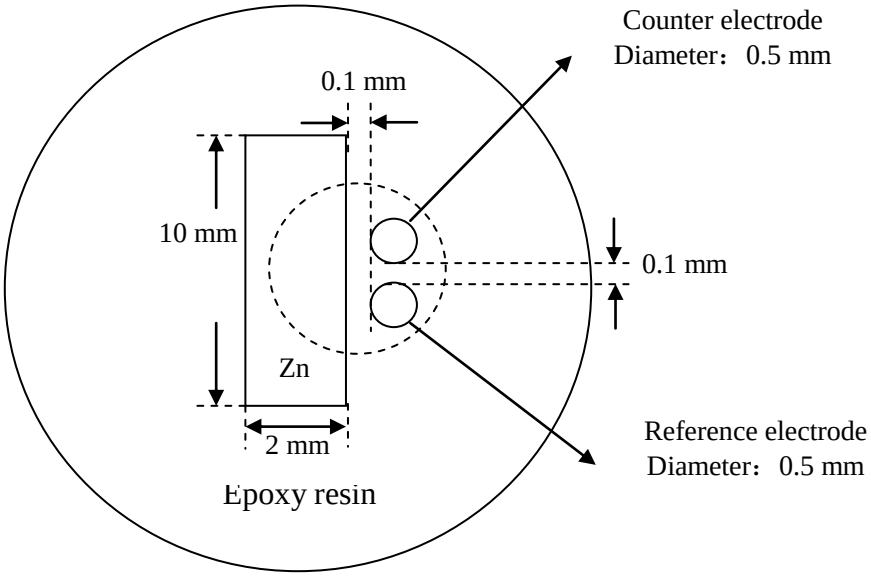

Figure 1. Schematic diagram of the Zn-Pt-Pt three-electrode system for the electrochemical tests of pure zinc under a NaCl electrolyte droplet.

A three-electrode system was established, and its schematic diagram is shown in Figure 1. A zinc plate and two identical pure Pt wires were embedded in epoxy resin. The zinc plate was of 99.99% purity and the exposed area of zinc for testing was 10 × 2 mm. The diameters of the Pt wires were 0.5 mm. The zinc plate served as a working electrode (WE), and the two identical pure Pt wires served as an RE and a counter electrode (CE). Three copper wires were welded with the three electrodes to ensure an electric connection for electrochemical measurements. The welded points were then sealed with epoxy. As shown in Figure 1, the distance between the zinc plate and these two Pt wires was 0.1 mm, and the distance between these two Pt wires was fixed at 0.1 mm. Before being ultrasonically cleaned in analytical grade ethanol for 5 min, this electrode system was wet ground with SiC paper down to 3000 grit and then polished with diamond paste down to 2 μm. Before testing, this electrode system was placed in a desiccator for 24 h. After NaCl particle was deposited in the central zone of the dotted circle (Figure 1), this three-electrode system was exposed to a chamber controlled at 97±1% RH and 25±0.1 ^{o}C for 2, 8 and 24 h. The electrode system was faced up in horizontal position. At each exposure condition three parallel samples were used.

All electrochemical measurements were conducted in a CHI660D electrochemical workstation. The pre-Tafel regions of polarisation were measured at -80 mV < E_{corr} < +50mV with a scan rate of 10 mV/s. R_p was determined by using the polarisation measurements of the current densities at the potential at -10 and 10 mV. EIS measurements were conducted at a frequency ranging from 100 kHz to 10 mHz at the open circuit potential (OCP) with a potential perturbation of ±5 mV.

3. RESULTS AND DISCUSSION

3.1. The feasibility of using Pt as an RE

It is well known that the mechanism of atmospheric corrosion is electrochemical in nature and the electrochemical test methods can be used to study the atmospheric corrosion process. However, it is very difficult to perform the electrochemical measurements using RE with Luggin capillary under a thin-electrolyte layer. The selection and placement of RE are critical in the application of electrochemical methods for investigating atmospheric corrosion of metals.

The conventional REs, which are most commonly used in Cl^--containing aqueous solutions, are the saturated calomel electrode and the silver-silver chloride (Ag/AgCl) electrode. However, these electrodes can act as sources for ionic contamination of the electrolyte solution absorbed on the metal surface. The leaking-induced contamination is mainly decided by the leak rate of the porous frit of the RE, which is generally designed on the order of 1 $\mu L\ h^{-1}$. A simple calculation listed in the following can show the significant effects of the chloride leaking-induced contamination [17]. Suppose the area of the electrode surface is 1 cm^2 and the electrolyte layer thickness on the top of the electrode is 1 mm, which is the maximum electrolyte layer thickness of the 'wet corrosion' defined by Tomashov model [18]. And consider a leaking rate of 1 $\mu L\ h^{-1}$, which is the lowest designed leaking rate of the porous frit of the RE, and chloride ion concentration of 4 M, which is the KCl concentration in a saturated calomel electrode. In a one-hour test, the initial chloride-free solution will develop a chloride concentration of 4×10^{-2} M. This chloride concentration will lead to the change of the atmospheric corrosion mechanisms of many metals. Thus, in order to avoid this risk, metallic RE must be developed for the application in the study of atmospheric corrosion processes of metals.

Cruz *et al* [19] and Tsutsumi *et al* [20] investigated the atmospheric corrosion of stainless steel under a chloride-containing thin-electrolyte layer using silver plate as a RE. The silver plate was galvanostatically polarized to produce Ag/AgCl in advance. Dubuisson *et al* [8] studied the corrosion behaviors of galvanized steel under an electrolytic drop by inserting two Pt wires, acted as RE and CE respectively, into the drop.

In the current study, two Pt wires were embedded at approximately 100 μm away from each other and from the WE in the epoxy resin. One of the Pt wires served as the RE and the other one acted as the CE. The design of this three-electrode system came from Ref. 8. Comparisons of the open circuit potentials of zinc and Pt with Ag/AgCl RE, and zinc with Pt RE were performed to verify the feasibility of using Pt as an RE. The experiments were conducted by using a 5.2-wt% NaCl bulk solution (with pH values ranging from 4 to 12) and a neutral NaCl bulk solution (with NaCl concentrations ranging from 3.5% to 26.5%). During the atmospheric corrosion process, the NaCl concentration and pH value were changed. Oxygen reduction in the cathodic regions led to an increase in pH value [21], while metal dissolution and hydrolysis of metallic ions in the anodic regions led to a decrease in pH value. Chloride ions participated in the corrosion reactions, which changed the chloride concentration with exposure time. The 5.2-wt% NaCl was selected because the deposited NaCl particles on the surface of the three-electrode system absorbed water from the ambient environment to form an electrolyte layer with a NaCl concentration of 5.2 wt% at 97% RH and 25 °C [22].

In this paper, $V_{Zn\text{-}Pt}$ represented the OCP of zinc in the three-electrode system relative to Pt RE whereas the OCP of zinc in the three-electrode system relative to real Ag/AgCl RE was referred to as $V_{Zn\text{-}Ag/AgCl}$. $V_{Pt\text{-}Ag/AgCl}$ stood for the OCP of Pt in the three-electrode system relative to real Ag/AgCl RE. The experimental results are shown in Figures 2 and 3. The results indicated that the OCPs of zinc relative to Pt RE, $V_{Zn\text{-}Pt}$, and relative to Ag/AgCl RE, $V_{Zn\text{-}Ag/AgCl}$, had similar change trends with pH and NaCl concentration.

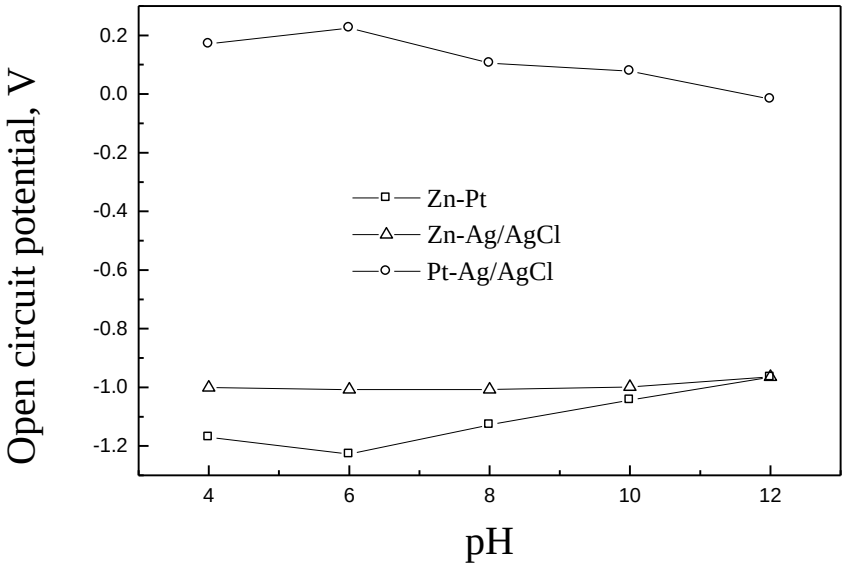

Figure 2. Variations of open circuit potential as a function of pH in 5.2-wt% NaCl solution at 25 ^{o}C.

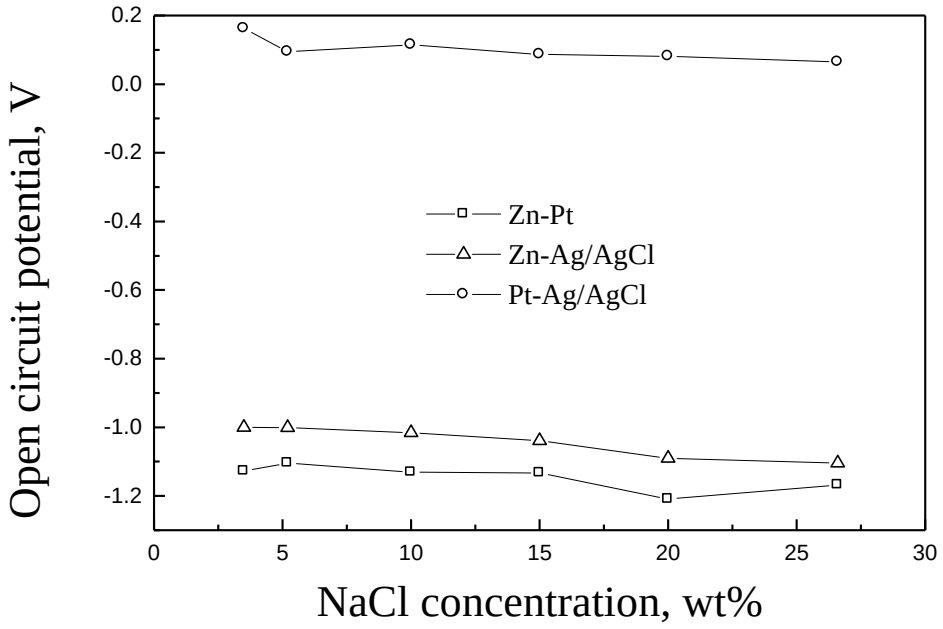

Figure 3. Variations of open circuit potential as a function of NaCl concentration in neutral solution at 25 ^{o}C.

The OCP measurement errors caused by replacing the Ag/AgCl reference with Pt are defined as follows:

$$\delta\% = \frac{V_{Zn-Pt} + V_{Pt-Ag/AgCl} - V_{Zn-Ag/AgCl}}{V_{Zn-Ag/AgCl}} \times 100\% \quad (1)$$

The calculation showed that the OCP measurements errors were lower than 3.5%. Pt is an inert metal which cannot be corroded. However, the potential of Pt varied with pH and NaCl concentration, as shown in Figures 2 and 3. Yet the potential of Pt was recognised as constant at least throughout each electrochemical measurement (short duration at less than 5 min). Hence, the DC polarisation that resulted from the potential change of RE during experimental measurements could be avoided. Slight changes in the electrolyte condition were expected in electrochemical tests. However, the changes in the Pt electrode potential could be calibrated according to Figures 2 and 3. Thus, the Pt electrode could be used as the RE for electrochemical tests.

3.2. Pre-Tafel region of polarisation measurements

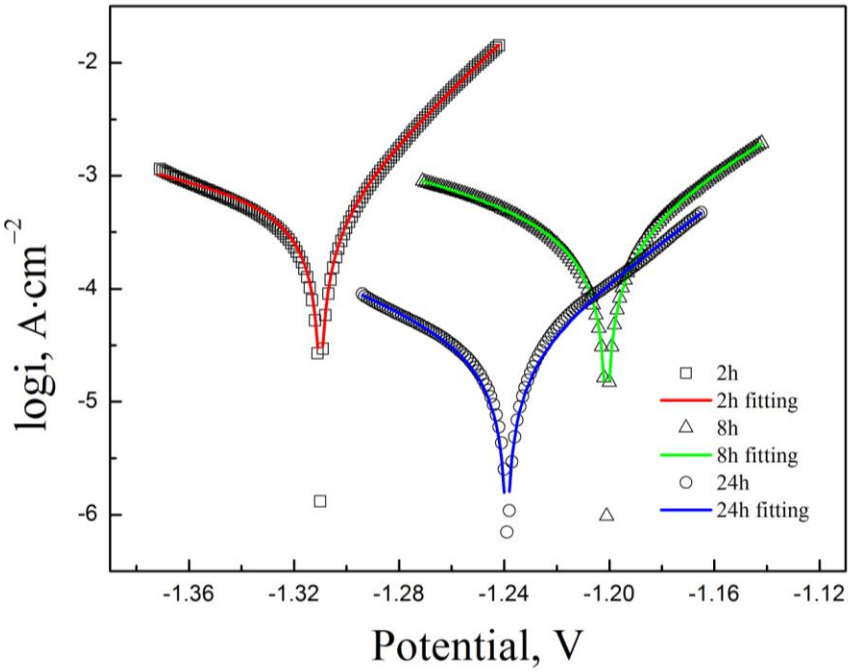

Figure 4. Experimental (dots with different symbols) and fitted (solid lines) potentiodynamic polarization curves in the vicinity of corrosion potential of zinc under a NaCl droplet after 2-, 8- and 24-h exposure at 97% RH and 25 ^{o}C.

Pre-Tafel regions of polarisation were measured and the results are shown in Figure 4. Different methods were employed to determine i_{corr}, B and R_p values from the pre-Tafel region in the vicinity of E_{corr}. One of them was the curve-fitting method which was based on Equation 2 that related

i to E

$$i = i_{corr}(e^{\frac{E-E_{corr}}{\beta_a}} - e^{-\frac{E-E_{corr}}{\beta_c}}) \quad (2)$$

Based on the best fit values of i_{corr}, β_a and β_c, B and R_p values were calculated according to Equations 3 and 4.

$$B = \frac{\beta_a \cdot \beta_c}{\beta_a + \beta_c} \quad (3)$$

$$R_p = \frac{B}{i_{corr}} \quad (4)$$

The solid lines in Figure 4 are the fitting curves of the pre-Tafel regions of the polarisation curves in the vicinity of E_{corr}. As shown in Figure 4, the measurements (dots with different symbols) were fitted very well.

The other method used in this paper combined linear polarisation and pre-Tafel region of polarisation. The principles of this method are as follows: First, R_p was calculated from the i values at $E\text{-}E_{corr} = \pm \Delta E_1$ (ΔE_1 usually takes 10 mV). It was supposed that the i value at $E\text{-}E_{corr} = +\Delta E_1$ was i_{+1} and the i value at $E\text{-}E_{corr} = -\Delta E_1$ was i_{-1}. The values of i_{+1} and i_{-1} were obtained from the polarisation curve. The R_p value can be calculated from the following equation:

$$R_p = \frac{2|\Delta E_1|}{|i_{+1}| + |i_{-1}|} \quad (5)$$

Second, it was supposed that the i value at $E\text{-}E_{corr} = +\Delta E_2$ was i_{+2} and the i value at $E\text{-}E_{corr} = -\Delta E_2$ was i_{-2}. ΔE_2 usually takes 40 mV. The values of i_{+2} and i_{-2} were obtained from the polarisation curve. Finally, the i_{corr} and B values were calculated as shown in the following equations:

$$i_{corr} \cong \frac{|\Delta E_2|}{2R_p\sqrt{6(\frac{R_p\sqrt{|i_{+2}|\cdot|i_{-2}|}}{|\Delta E_2|} - 1)}} \quad (6)$$

$$B \cong \frac{|\Delta E_2|}{2\sqrt{6(\frac{R_p\sqrt{|i_{+2}|\cdot|i_{-2}|}}{|\Delta E_2|} - 1)}} \quad (7)$$

Detailed information is given in Ref. 23, and the calculated results are listed in Table 1. As shown in Table 1, the fitted values obtained from these two methods are essentially similar. These

results verified that the data was analysed correctly.

Table 1. i_{corr}, B and R_p values obtained from different analysis methods of zinc under a NaCl droplet after 2-, 8- and 24-h exposure at 97% RH and 25 ^{o}C. Method 1 is the curve fitting method, and Method 2 is the method combining linear polarisation and pre-Tafel region of polarisation.

	$i_{corr}(uA \cdot cm^{-2})$			$B(mV)$			$R_p(\Omega \cdot cm^2)$		
	2h	*8h*	*24h*	*2h*	*8h*	*24h*	*2h*	*8h*	*24h*
Method1	311.66	218.76	23.77	15.32	19.20	13.92	69.20	120.90	582.30
Method2	291.38	232.40	50.82	15.14	19.68	24.19	66.43	121.18	471.54

As shown in Table 1, i_{corr} decreased with exposure time and R_p increased with exposure time.

3.3. EIS measurements

EIS can provide a non-destructive assessment of the corrosion behaviors and can study the corrosion mechanism. EIS measurements of the electrode after 2-, 8-, and 24-h exposure under a NaCl electrolyte droplet were performed and the results are shown in Figure 5. The dots with different symbols are the measurements, and the solid lines are fitted curves. The Nyquist plot in Figure 5 showed two apparent capacitive arcs after 2- and 8-h exposure. After 24-h exposure, the Nyquist plot exhibited obvious Warburg impedance in the low frequency region, which revealed that a diffusion-controlled corrosion process occurred on the zinc surface. This diffusion process could be attributed to the formation of insoluble corrosion products, which blocked the mass transfer process of the corrosion reactions.

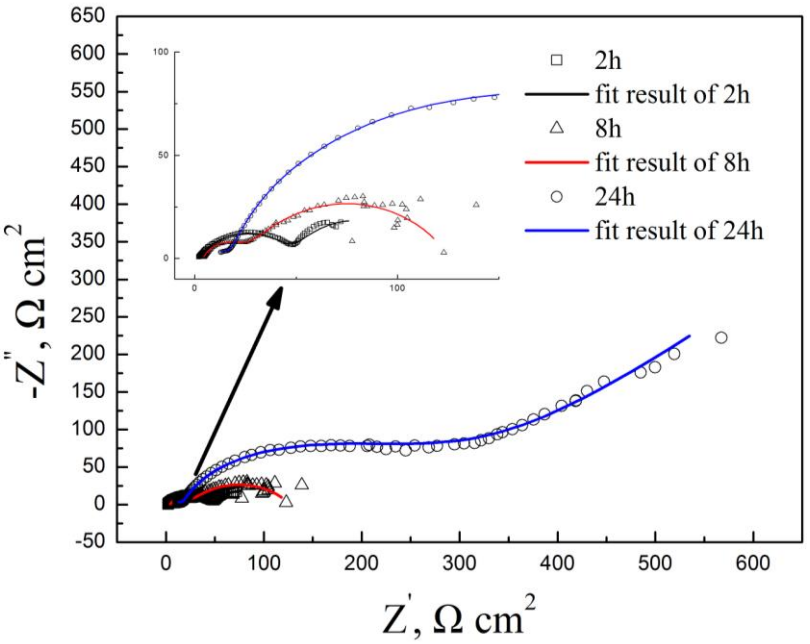

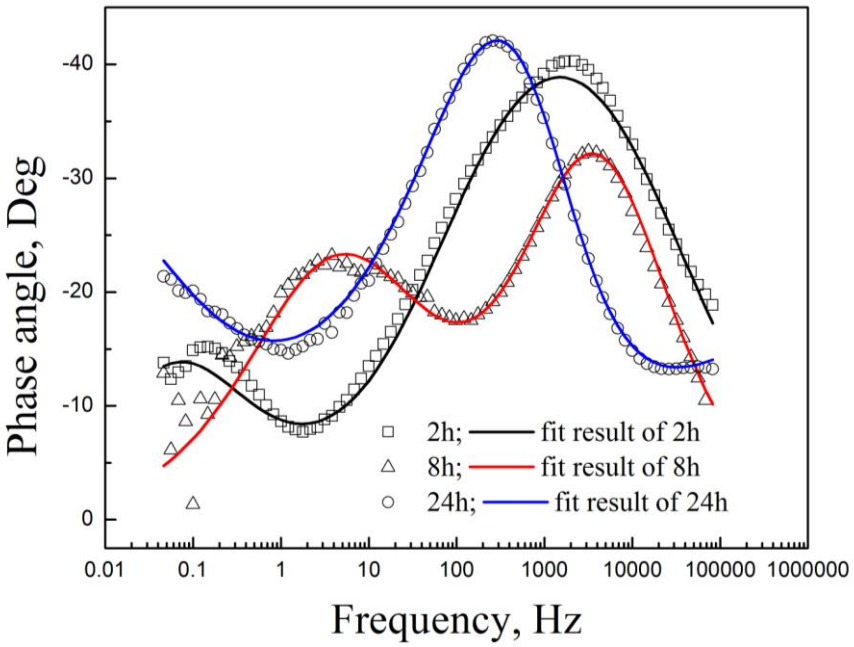

Figure 5. Experimental (dots with different symbols) and fitted (solid lines) Nyquist plots and Bode phase angle plots for zinc under the NaCl droplet after 2-, 8- and 24-h exposure at 97% RH and 25 ^{o}C.

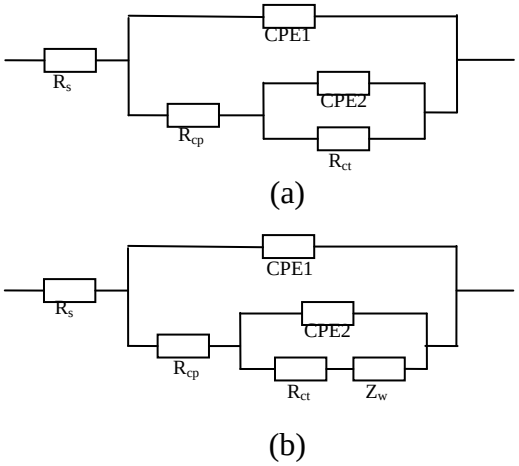

Figure 6. Equivalent circuits used for fitting the EIS data of pure zinc under a NaCl electrolyte droplet after different exposure time at 97% RH and 25 ^{o}C. R_s was the solution resistance; R_{cp} and CPE1 were the resistance and capacitance of the corrosion products, respectively; R_{ct} and CPE2 were the charge transfer resistance and the double layer capacitance of the corrosion reactions, respectively; Z_W was the Warburg impedance. (a) without displaying the Warburg impedance, (b) with displaying the Warburg impedance.

The angular value of the line which corresponded to the Warburg impedance in the low frequency region of the Nyquist plot was lower than $\pi/4$. A possible reason is that the insoluble corrosion products (which was formed on the zinc surface) roughened the electrode surface, resulted in a diffusion process which partially equivalent to a spherical diffusion process, and decreased the

angular value.

According to the EIS data and the NaCl-induced atmospheric corrosion process of zinc, two equivalent circuits (Figure 6) were established to fit the EIS results obtained after different exposure durations. Figure 6a was used to fit the EIS data after 2- and 8-h exposure and Figure 6b was used to fit the EIS data after 24-h of exposure. R_s was the solution resistance; CPE1 and R_{cp} were the capacitance and resistance of the insoluble corrosion products formed during exposure, respectively. CPE2 and R_{ct} were the double-layered capacitance and the charge transfer resistance of the corrosion reactions, respectively. Z_w was the Warburg impedance. CPE1 and CPE2 were constant phase angle elements. Their impedance was equal to $(Y_0(j\omega)^n)^{-1}$, where ω was the ac-voltage angular frequency (rad s^{-1}), and Y_0 and n were the frequency-independent parameters.

Figure 5 shows the experimental and the fitted results. The two equivalent circuits fit the experimental results well in most of the frequency range, which indicated that the given equivalent circuits were suitable for interpreting the initial NaCl-induced corrosion behaviours of zinc. Table 2 shows the fitted parameters of the EIS of zinc under the NaCl droplet after 2-, 8- and 24-h exposure in 97% RH and 25 °C.

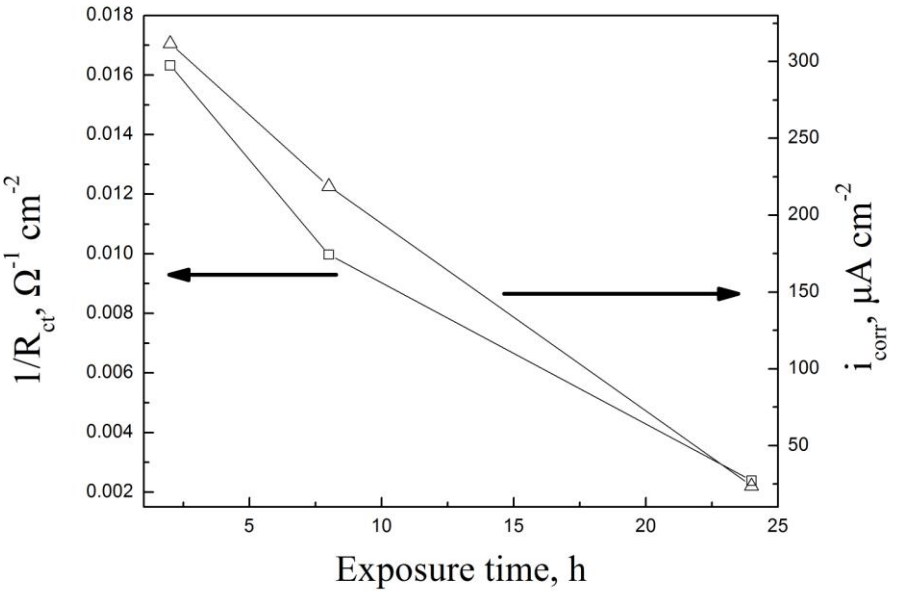

Figure 7. i_{corr} obtained from curve fitting of pre-Tafel region of polarisation curves and $1/R_{ct}$ obtained from electrochemical impedance spectroscopy as a function of exposure time for zinc under the NaCl electrolyte droplet at 97%RH and 25 ^oC.

As reported in a previous study [24], using R_{ct} to define the corrosion rate was significantly more accurate than using R_p. R_{ct} was simply determined by the faradic process of the charge transfer controlled corrosion. However, a large error will present itself when R_p was calculated from the impedance diagram which had more than one time constant. In the present study, the reciprocal of R_{ct}, which was obtained from Table 2, was used as a parameter to evaluate the corrosion rate, as shown in

Figure 7. $1/R_{ct}$ and i_{corr} have similar change trends with exposure time, and this confirms the correctness of the polarisation data and the selected equivalent circuits from another side.

R_p can also be determined from EIS measurements by subtracting the high frequency impedance at 10 kHz from the low frequency impedance at 10 mHz [19]. In the present study, the R_ps obtained from EIS measurements and from the curve-fitting results of the pre-Tafel region of polarisation are shown in Figure 8. As shown in Figure 8, the R_ps obtained by using these two methods are in great agreement, which indicates that the pre-Tafel region of the polarisation can be used to study the corrosion behaviours of zinc.

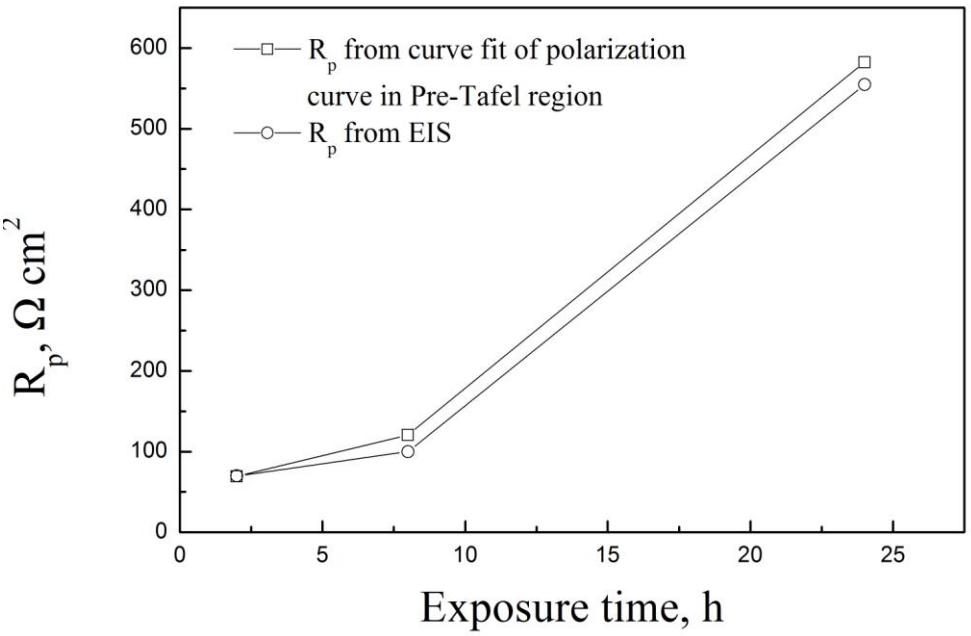

Figure 8. Changes of R_p with exposure time; R_p was obtained from curve fitting of the pre-Tafel region of polarisation curves and from EIS data, respectively.

Table 2. Fitted parameters of the EIS of zinc under a NaCl droplet after 2-, 8- and 24-h exposure at 97% RH and 25 ^{o}C.

Fitted Parameters	*2h*	*8h*	*24h*
R_s ($\Omega \cdot cm^2$)	1.513	4.053	1.002E-7
$(Y_0)_1$ ($uF \cdot cm^{-2} \cdot Hz^{1-n1}$)	525.3	68.71	613.3
n_1	0.5923	0.7369	0.3092
R_{cp} ($\Omega \cdot cm^2$)	48.13	22.13	24.93
$(Y_0)_2$ ($uF \cdot cm^{-2} \cdot Hz^{1-n2}$)	4.31E+4	2.86E+3	23.95
n_2	0.6662	0.6042	0.8293
R_{ct} ($\Omega \cdot cm^2$)	61.24	100.3	418.9
Z_W ($uF \cdot cm^{-2} \cdot Hz^{0.5}$)	-	-	4.785E+3

4. CONCLUSIONS

In the present paper, the initial NaCl particles induced corrosion of pure zinc under a droplet had been studied by employing a three-electrode cell system in electrochemical tests. The feasibility of using Pt as RE was studied and the errors of the potential measurements using Pt RE were analysed. The pre-Tafel regions of the polarisation curves and EIS were measured and analysed.

The main conclusions can be drawn in the following:

(1). This paper developed a three-electrode system, Zn-Pt-Pt. These three electrodes were 0.1 mm apart. This configuration minimised the resistance polarisation between the WE and the CE and the solution resistance between the WE and the RE. Thus, the proposed three-electrode system can be used to investigate the atmospheric corrosion of zinc covered by a thin-electrolyte layer.

(2). Pt can be used as an RE for electrochemical tests, and the errors of the potential measurements using Pt RE were lower than 3.5%.

(3). Curve-fitting method and the method combining linear polarisation with pre-Tafel region of polarisation were feasible to analyse the polarisation curves in the vicinity of E_{corr}. These two methods were consistent with each other.

(4). Corrosion rate decreased with exposure time. The electrode process was changed from the original charge transport control to the joint control of charge transport and mass transport. This change was attributed to the formation of insoluble corrosion products with exposure time, which hindered the mass transfer process of corrosion reactions.

(5). $1/R_{ct}$ had a trend similar to i_{corr} in relation to exposure time.

(6). R_p obtained from the polarisation curve in the vicinity of E_{corr} was consistent with that from EIS.

ACKNOWLEDGEMENT
This work was financially supported by the Hundreds-Talent Program of the Chinese Academy of Sciences (Y02616101L).

References

1. I.S. Cole, W.D. Ganther, S.A. Furman, T.H. Muster, A.K. Neufeld, *Corros. Sci*. 52 (2010) 848.
2. I.S. Cole, T.H. Muster, S.A. Furman, N. Wright, A. Bradbury, *J. Electrochem. Soc*. 155 (2008) C244.
3. A.P. Yadav, H. Katayama, K. Noda, H. Masuda, A. Nishikata, T. Tsuru, *Electrochim. Acta* 52 (2007) 3121.
4. T.E. Graedel, *J. Electrochem. Soc*. 136 (1989) 193C.
5. P. Qiu, D. Persson, C. Leygraf, *J. Electrochem. Soc*. 156 (2009) C81.
6. A.K. Neufeld, I.S. Cole, A.M. Bode, S.A. Furman, *Corros. Sci.* 44 (2002) 555.
7. Z.Y. Chen, D. Persson, C. Leygraf, *Corros. Sci*. 50 (2008) 111.
8. E. Dubuisson, P. Lavie, F. Dalard, J. Caire, S. Szunerits, *Corros. Sci*. 49 (2007) 910.
9. Y.Y. Chen, S.C. Chung, H.C. Shih, *Corros. Sci*. 48 (2006) 3547.
10. T. Falk, J.E. Svensson, L.G. Johansson, *J. Electrochem. Soc*. 145 (1998) 2993.

11. T.H. Muster, A. Bradbury, A. Trinchi, I.S. Cole, T. Markley, D. Lau, S. Dligatch, A. Bendavid, P. Martin, *Electrochim. Acta* 56 (2011) 1866.
12. T. Tsuru, K.I. Tamiya, A. Nishikata, *Electrochim. Acta* 49 (2004) 2709.
13. A.P. Yadav, F. Suzuki, A. Nishikata, T. Tsuru, *Electrochim. Acta* 49 (2004) 2725.
14. S. Yee, R.A. Oriani, M. Stratmann, *J. Electrochem. Soc*. 138 (1991) 55.
15. A. Nishikata, Y. Ichihara, T. Tsuru, *Electrochim. Acta* 41 (1996) 1057.
16. X.N. Liao, F.H. Cao, L.Y. Zheng, W.J. Liu, A.N. Chen, J.Q. Zhang, C.N. Cao, *Corros. Sci*. 53 (2011) 3289.
17. R.G. Kelly, J.R. Scully, D.W. Shoesmith, R.G. Buchheit, Electrochemical Techniques in Corrosion Science and Engineering, Marcel Dekker Inc., New York, pp.15 (2003).
18. N.D.Tomashov, *Corrosion* 20 (1964) 7.
19. R.P.Vera Cruz, A. Nishikata, T. Tsuru, *Corros. Sci*. 38 (1996) 1397.
20. Y. Tsutsumi, A. Nishikata, T. Tsuru, *J. Electrochem. Soc*. 152 (2005) B358.
21. M.B.Vukmirovic, N.Dimitrov, K. Sieradzki, *J. Electrochem. Soc*. 149 (2002) B428.
22. Z.Y. Chen, R.G. Kelly, *J. Electrochem. Soc*. 157 (2010) C69.
23. C.N. Cao, J.Q. Zhang, An Introduction to Electrochemical Impedance Spectroscopy, Chinese Science Press, Beijing, pp.145 (2002).
24. Y.L. Cheng, Z. Zhang, F.H. Cao, J.F. Li, J.Q. Zhang, J.M. Wang, *Corros. Sci*. 46 (2004) 1649.